

# Temperature Field Determination during Bridge Pier Construction

**Ba-Thang Phung**

Faculty of Civil Engineering, University of Transport Technology, Trieu Khuc, Thanh Xuan, Hanoi, Vietnam  
thangpb@utt.edu.vn

**Trong Chuc Nguyen**

Institute of Techniques for Special Engineering, Le Quy Don Technical University, Hanoi, Vietnam  
trongchuc.nguyen@lqdtu.edu.vn (corresponding author)

Received: 1 January 2025 | Revised: 14 January 2025 | Accepted: 18 January 2025

Licensed under a CC-BY 4.0 license | Copyright (c) by the authors | DOI: <https://doi.org/10.48084/etasr.9265>

## ABSTRACT

Thermal deformation resulting from the hydration of cement in the concrete mix is a primary cause of thermal cracking in structures, particularly in mass concrete elements, and more specifically in the abutments and piers of bridges. These cracks are most likely to occur at an early age, when the temperature rise within the concrete is most pronounced. The formation of thermal cracks is especially problematic in the early stages of construction, as the temperature differential between the interior and surface of the structure can lead to significant stresses. Therefore, understanding the temperature and stress fields during the construction of bridge piers is crucial for identifying effective strategies to mitigate thermal cracking. This paper investigates the underlying causes of thermal crack formation in bridge piers and applies the Finite Element Method (FEM) to analyze the temperature field during the construction process under typical Vietnamese conditions. The findings of this study aim to provide practical solutions for preventing thermal cracking in bridge pier structures during the construction phase, ensuring the durability and integrity of the bridge over time.

*Keywords-thermo-mechanical properties; temperature field; thermal crack; crack risk; mass concrete*

## I. INTRODUCTION

According to the American Concrete Institute's definition of mass concrete, any mass of concrete of sufficiently large volume requires control measures for the increase in heat due to the thermal hydration of cement and volume change to minimize the possibility of cracks forming. Examples of structures that use concrete of considerable volume include the foundations of high-rise buildings, thermal power plants, bridges, roads, waterworks, and other infrastructure. The dimensions of large concrete blocks are subject to restrictions that are contingent upon the national standards. Nonetheless, the American Concrete Association (ACA) advises taking precautions to avoid crack formation for any one-dimensional structure larger than one meter [1-2]. Concurrently, a significant number of Russian scientists are exploring the potential for an expedited evaluation of the crack formation in mass concrete structures. According to studies, the temperature differential between a concrete block's surface and its center cannot exceed 200 °C [3, 4]. In Vietnam, large blocks are categorized as concrete or reinforced concrete structures that attain sufficient size to generate tensile stress as a consequence of the cement's thermal hydration effect (TCVN: 9341-2012 standards). It is imperative to note that concrete is susceptible to fracture and cracking if its tensile limit is exceeded,

underscoring the necessity for meticulous precautions to avert such outcomes. The stress-strain state of mass concrete during construction is influenced by various factors, including the thermal load [5-7]. A multitude of parameters, involving base temperature, air temperature, wind speed, heat radiation intensity, and cement type, collectively influence the thermal regime in mass concrete [3]. Of particular significance is the heat of hydration that the cement generates. Additionally, the dimensions of the used mixture, maintenance practices, and the progression of construction can also influence the heat distribution within mass concrete. Consequently, a substantial temperature disparity between the core and the surface of the concrete mass is observed during the construction phase, leading to the formation of tensile stress. This stress, if sufficiently large and surpassing the tensile capacity of the concrete at the construction site, results in the onset of tensile stress. The occurrence of thermal cracks is a consequence of the early age [4-6]. To mitigate the risk of thermal cracking, it is recommended that the temperature difference ( $\Delta T$ ) be maintained below 20 °C [7]. Early-stage thermal cracking poses a threat to the integrity of the structure. It is therefore imperative to identify such situations promptly and implement measures to mitigate or reduce their likelihood. It is essential to acknowledge the significance of preventing thermal cracking

and to implement the necessary measures at the outset. A multitude of methods are currently available to prevent thermal cracking in the early stages of construction, including the use of insulated formwork, the fragmentation of the poured mass into smaller components, the reduction of the concrete mixture temperature, and the substitution of fly ash for a greater proportion of cement. Other strategies include the usage of a cooling pipe system or the mitigation of the pour's exposure to solar radiation.

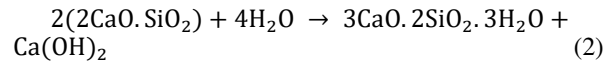
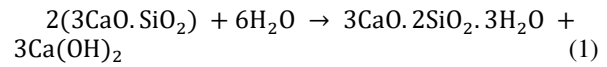
A considerable number of experts, both domestic and foreign, have expressed consistent concerns regarding the issue of cracked bridge piers and have conducted extensive research on the subject. The inspection report, authored by the Ministry of Construction experts, identifies two primary factors contributing to the cracking of pier T22 on the Vinh Tuy bridge. These factors are: the primary cause is attributed to the Vinh Tuy bridge's pier being constructed with a substantial concrete structure. Consequently, a substantial amount of heat was generated from the cement hydro-pyromic reaction within the poured mass during construction, and no measures were implemented to mitigate this. The second cause is the high temperature differential and generation of poured concrete blocks at high temperatures. The phenomenon of thermal stress and variations in deformation are attributed to the presence of temperature variations both within and between the poured blocks. When the thermal stress exceeds the concrete's tensile strength, the cylindrical concrete undergoes cracking. The phenomenon is attributed to a combination of factors, including concrete creep under the influence of regular loads during exploitation and use, temperature changes, humidity in the environment, and shrinkage over time. This combination of factors leads to the widening of the crack. Preventing the formation of thermal cracks during the early stages of bridge pier construction is a key area of interest and research for scientists. This study uses the Midas Civil program to analyze the development of the temperature field within a concrete block, taking into account factors, such as the cement content, initial temperature variations of the poured block, and various formwork methods.

## II. MATERIALS AND METHODS

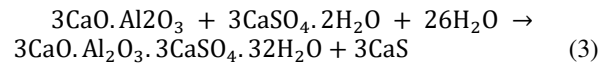
### A. Research Subjects

The present paper is an analytical study of the temperature fields in a reinforced concrete bridge pier. The dimensions of the bridge piers are: the foundation body measures 4 m × 2 m × 6 m and is located on a ground area of 12 m × 15 m × 5 m, while the foundation pedestal has dimensions of 7 m × 6 m × 2.5 m. Figure 1 provides a visual representation of the concrete block's dimensions. Assuming an average daily ambient temperature of 25 °C, the foundation temperature is set at 25 °C. The hydration process of the constituent minerals in cement results in the production of heat. The measurement and monitoring of the heat produced can be facilitated by employing an isotherm. The heat flow during cement hydration can be subdivided into five stages. In Figure 2, a standard hydration process is depicted. In addition to describing and characterizing the cement's setting and curing processes, data from studies on the heat of hydration of cement can be also used to forecast the development of heat in concrete [8, 9]. The

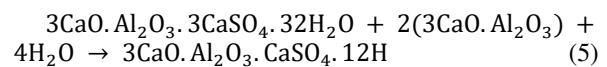
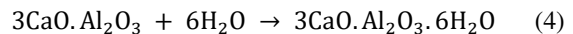
hydration reaction between the four most significant minerals of cement and water is expressed through (1)-(6) [9]:



When the cement composition has enough gypsum:



When the cement composition does not contain enough gypsum:



Mineral hydration  $\text{C}_4\text{AF}$ :

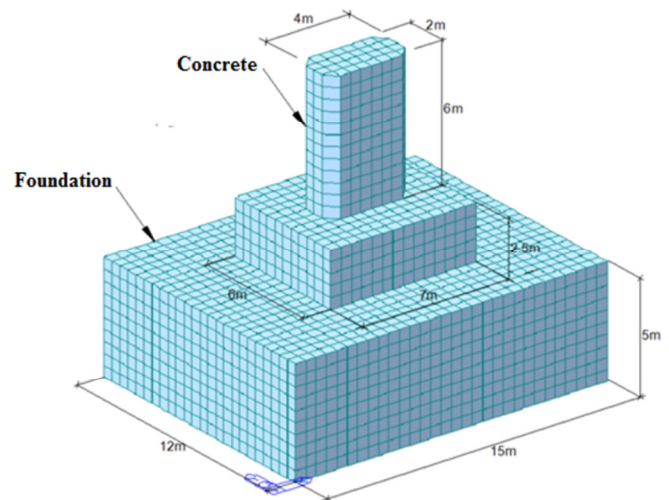
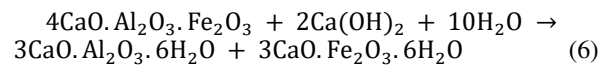


Fig. 1. Reinforced concrete bridge pier model used for analysis.

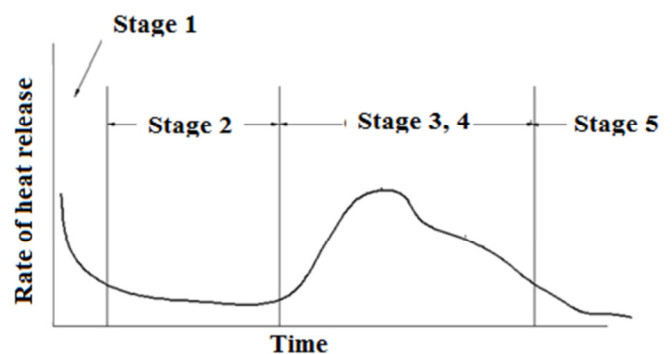


Fig. 2. Heat release rate during hydration of Portland cement.

The temperature at the center of the concrete mass under adiabatic conditions is experimentally determined according to:

$$Q(t) = Q_{\infty} \cdot \left[ 1 - e^{-r_{AT} \cdot (t-t_{0,Q})^{s_{AT}}} \right] \quad (7)$$

where:  $t$  is the age of concrete in days,  $Q(t) = T_{ad}$  is the adiabatic temperature of concrete at an age of  $t$  days in  $^{\circ}\text{C}$ ,  $Q_{\infty}$  is the maximum temperature of concrete under adiabatic conditions in  $^{\circ}\text{C}$ ,  $r_{AT}$ ,  $s_{AT}$  are the parameters showing the rate of temperature change and  $t_{0,Q}$  is the age when concrete begins to heat up in days. The quantities  $Q_{\infty}$ ,  $r_{AT}$ ,  $s_{AT}$ ,  $t_{0,Q}$  in (7) are set as a function of the concrete temperature when pouring and the cement content changes from  $400 \text{ kg/m}^3 \div 550 \text{ kg/m}^3$  to be calculated, as illustrated in Table I. The physical and mechanical properties of concrete and soil are presented in Table II.

TABLE I. CALCULATION PARAMETERS

Parameters	$W_c: 400 \text{ kg/m}^3 < W_c \leq 550 \text{ kg/m}^3$	
$Q_{\infty} = a_{AT} + b_{AT} \times T_a$	$a_{AT} = 40.0 + 0.057 \times W_c$	$b_{AT} = -0.146 + 3.08 \times 10^{-4} \times \frac{W_c}{W_c}$
$r_{AT} = a_{AT} + b_{AT} \times T_a$	$a_{AT} = -0.426 + 2.07 \times 10^{-3} \times \frac{W_c}{W_c}$	$b_{AT} = 0.0471 + 1.88 \times 10^{-3} \times \frac{W_c}{W_c}$
$s_{AT} = 1$		
$t_{0,Q} = a_{AT} \times \exp(-b_{AT} \times T_a)$	$a_{AT} = 0.832 - 5.31 \times 10^{-4} \times \frac{W_c}{W_c}$	$b_{AT} = 0.0482 + 6.8 \times 10^{-3} \times \frac{W_c}{W_c}$

TABLE II. CALCULATED PARAMETERS OF MATERIALS USED IN ANALYSIS

TT	Parameters	Concrete	Foundation
1	Thermal conductivity coefficient, $\text{W}/(\text{m}^{\circ}\text{C})$	2.31	3.59
2	Specific heat, $\text{kJ}/(\text{kg}^{\circ}\text{C})$	0.96	0.85
3	Specific weight, $\text{kg}/\text{m}^3$	2,400	1,800
4	Convective heat transfer coefficient, $(\text{W}/\text{m}^2^{\circ}\text{C})$	13.94	14.0
5	Thermal expansion coefficient, $1/^{\circ}\text{C}$	$1.0 \times 10^{-5}$	$1.0 \times 10^{-5}$
6	Poatxong coefficient	0.2	0.25
7	Cement content, $\text{kg}/\text{m}^3$	400÷550	-
8	Initial temperature of concrete mixture, $^{\circ}\text{C}$	10÷30	25

B. FEM to Solve Heat Problems

The three-dimensional heat transfer process in an anisotropic medium is described by [11]:

$$\rho C \frac{\partial T}{\partial t} = \frac{\partial}{\partial x} \left( \lambda_x \frac{\partial T}{\partial x} \right) + \frac{\partial}{\partial y} \left( \lambda_y \frac{\partial T}{\partial y} \right) + \frac{\partial}{\partial z} \left( \lambda_z \frac{\partial T}{\partial z} \right) + q \quad (8)$$

where:  $\rho$  is the volume of concrete in  $\text{kg}/\text{m}^3$ ,  $C$  is the specific heat of concrete in  $\text{kcal}/\text{kg}^{\circ}\text{C}$ ,  $T(x,y,z,t)$  is the temperature at coordinates  $(x,y,z)$  at time  $t$  in  $^{\circ}\text{C}$ ,  $\lambda_x, \lambda_y, \lambda_z$  are the thermal conductivity coefficient of the material in  $x,y,z$  directions, and  $q$  is the heat generated in a unit volume in  $\text{kcal}/\text{m}^3$ .

1) Boundary Conditions

At the boundary the temperature remains constant:

$$T = T_0, T(x, y, z, t) = T_0 \text{ with } t > 0 \quad (9)$$

At the heat transfer boundary:

$$\lambda_x \frac{\partial T}{\partial x} n_x + \lambda_y \frac{\partial T}{\partial y} n_y + \lambda_z \frac{\partial T}{\partial z} n_z + q(t) = 0, t > 0 \quad (10)$$

At the convection boundary:

$$\lambda_x \frac{\partial T}{\partial x} n_x + \lambda_y \frac{\partial T}{\partial y} n_y + \lambda_z \frac{\partial T}{\partial z} n_z + h_c(T - T_{\infty}) = 0, t > 0 \quad (11)$$

where:  $n_x; n_y; n_z$  indicate the direction of the heat transfer surface under consideration,  $q(t)$  is the heat generated in a unit volume at time  $t$  in  $\text{kcal}/\text{m}^3$ ,  $h_c$  is the convection coefficient in  $\text{kcal}/\text{m}^2 \text{ h}^{\circ}\text{C}$ , and  $T_{\infty}$  is the temperature at the convection surface in  $^{\circ}\text{C}$ . The FEM for solving the problem of unsteady heat transfer and internal sources is represented by [12, 13]:

$$[K]\{T\} + [C] \left\{ \frac{\partial T}{\partial t} \right\} = [Q], t > 0 \quad (12)$$

where  $[C] = \int_V \rho \cdot c \cdot [N]^T [N] dV$  is the specific heat matrix,  $[N]$  is the function matrix,  $[N]^T$  is the inverse matrix,  $[K]$  is the thermal conductivity coefficient matrix with  $[K] = \int_V [B]^T [D] [B] dV + \int_S h [N]^T [N] dS$ , where:

$$[D] = \begin{pmatrix} k_x & 0 & 0 \\ 0 & k_y & 0 \\ 0 & 0 & k_z \end{pmatrix}, [B] = \begin{pmatrix} \frac{\partial N_1}{\partial x} & \frac{\partial N_2}{\partial x} \\ \frac{\partial N_1}{\partial y} & \frac{\partial N_2}{\partial y} \\ \frac{\partial N_1}{\partial z} & \frac{\partial N_2}{\partial z} \end{pmatrix}$$

$$[Q] = \int_V q_v [N]^T dV - \int_S q [N]^T dS + \int_S h [N]^T T_K dS \quad \text{and} \quad T = \sum N_i T_i = [N] \cdot \{T\}$$

2) Structural Discretization

The structural discretization process is a critical component of the analysis, and it is essential to understand its implications for the overall model. This is achieved through the implementation of the Galerkin method or the variational method [15].

3) Discrete Time Based on Galerkin Method

$$I(t) = \frac{1}{2} \int_V \left[ k_x \left( \frac{\partial T}{\partial x} \right)^2 + k_y \left( \frac{\partial T}{\partial y} \right)^2 + k_z \left( \frac{\partial T}{\partial z} \right)^2 - 2q_v T \right] dV + \int_{S_2} q T dS + \int_{S_2} \frac{1}{2} h (T - T_a)^2 dS \quad (13)$$

In order to solve the unstable heat transfer problem, it is necessary to analyze the time in the following:

$$\left\{ \frac{\partial T}{\partial t} \right\} = \frac{1}{\Delta t} [\{T(t_n) - T(t_{n-1})\}] \quad (14)$$

Equation (14) can be rewritten as:

$$[K]\{T\} + \frac{[C]}{\Delta t} [\{T(t_n) - T(t_{n-1})\}] = [Q] \quad (15)$$

where:  $[Q]$  is the heat matrix generated and  $\Delta t = \Delta t_n - \Delta t_{n-1}$  is the step of calculation time. The solution of (15) provides the temperature field in the concrete block at various times. Currently, there are numerous structural analysis software programs that use the PTHH method and are capable of analyzing temperature and stress: these include ANSYS, ABAQUS, and MIDAS. In this study, the Midas Civil software is employed to analyze the temperature field in large concrete structures [15-18].

III. RESULTS AND DISCUSSION

A. Effect of Cement Content

This study examines scenarios in which the cement content varies between  $400 \text{ kg}/\text{m}^3$  and  $550 \text{ kg}/\text{m}^3$ . Its objective is to

ascertain the impact of the cement content on the maximum temperature and maximum temperature difference in bridge pier structures. Table III displays the temperature difference ( $\Delta T$ ) between the surface and the center after applying the FEM to determine the maximum temperature value ( $T_{max}$ ). The values of  $T_{max}$  and  $\Delta T$  both increase with an increasing cement content. As the cement content increases from 400 kg/m<sup>3</sup> to 550 kg/m<sup>3</sup>, the value of  $T_{max}$  increases by 12.46% and the value of  $\Delta T$  increases by 17.46%.

TABLE III. EFFECT OF CEMENT CONTENT ON MAXIMUM TEMPERATURE AND MAXIMUM TEMPERATURE DIFFERENCE IN BRIDGE PIER STRUCTURES

Cement content (kg/m <sup>3</sup> )	400	430	460	490	520	550
$T_{max}$ (°C)	87.85	90.12	92.35	94.54	96.68	98.80
$\Delta T$ (°C)	47.52	49.23	50.91	52.57	54.20	55.82

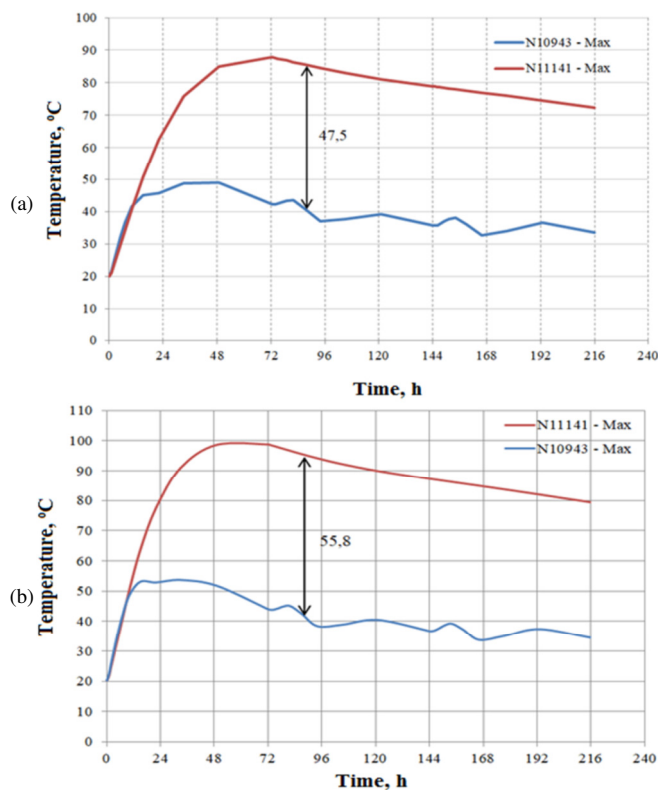


Fig. 3. Temperature evolution at the survey point at the center and surface of the bridge pier with different cement content (N10943: surface of the bridge pier, N11141: center of the bridge pier), (a) 400 kg/m<sup>3</sup>, (b) 550 kg/m<sup>3</sup>.

The increase in heat production resulting from the elevated cement content, due to the process of cement hydration, can be attributed to the rise in temperature of the concrete block's center and the consequent increase in the temperature differential between the center and the surface of the block. It has been observed that the concrete structure generates a substantial amount of heat, despite the variation in cement content ranging from 400 kg/m<sup>3</sup> to 550 kg/m<sup>3</sup>. The disparity in temperatures between the surface and center of the concrete block is not permissible, as it increases the likelihood of concrete cracking. To mitigate this risk, it is essential to employ suitable material solutions and take measures to

prevent thermal cracks during construction. As depicted in Figure 3, the temperature field in the bridge piers demonstrates the thermal evolution in two scenarios: minimum cement content and maximum cement content in 1 m<sup>3</sup> of concrete mixture.

B. Influence of the Initial Temperature of Concrete Mixture

This article analyzes scenarios in which the initial temperature of a concrete mixture is altered from 100 °C to 300 °C. Table IV presents the outcomes of a finite element analysis conducted on the temperature field of a bridge pier structure.

TABLE IV. EFFECT OF INITIAL TEMPERATURE ON MAXIMUM TEMPERATURE AND MAXIMUM TEMPERATURE DIFFERENCE

$T_{init}$	10	14	18	22	26	30
$T_{max}$ (°C)	83.44	87.01	91.48	95.30	99.99	104.6
$\Delta T$ (°C)	42.79	46.88	50.23	53.18	55.91	58.53

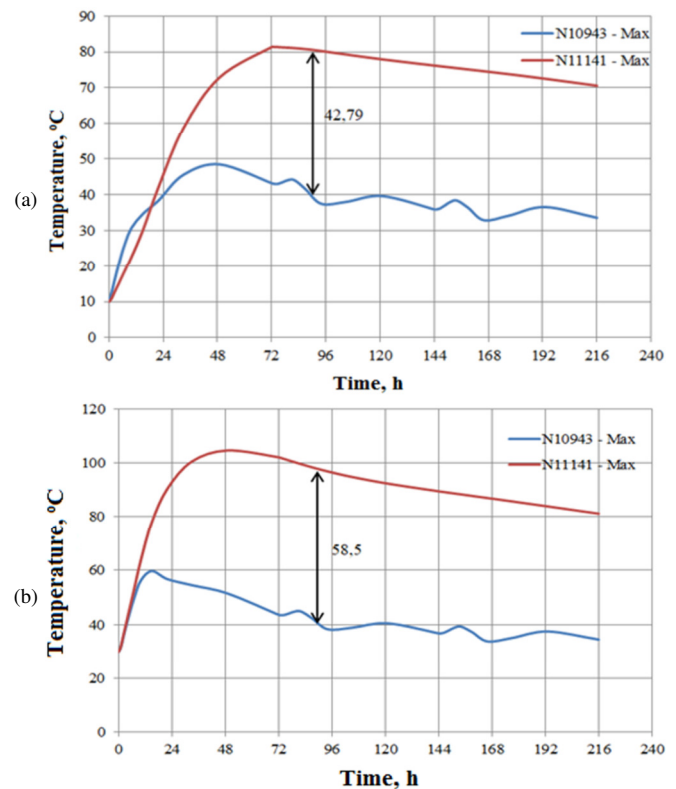


Fig. 4. Temperature evolution at the survey point at the center and surface of the bridge pier with the initial temperature cases of: (a) 10°C and (b) 30°C. (N10943: surface of the bridge pier, N11141: center of the bridge pier).

The findings indicate that the temperature distribution within the concrete mass is significantly influenced by the initial temperature of the poured mixture. Specifically, an increase in the initial temperature of the concrete results in a corresponding increase in the temperature at the center of the concrete block, and vice versa. It is evident that a 1 °C rise in the concrete mixture's initial temperature leads to a 1 °C increase in the maximum temperature within the bridge pier

structure. Figure 4 demonstrates the temperature variation at the surface and center of bridge piers as the initial concrete mixture temperature is changed.

C. Influence of the Formwork Type Used

This paper analyzes the impact of steel and wooden formwork on the temperature distribution within bridge pier structures. The convection coefficients for each type of formwork are: steel formwork 12 kcal/m<sup>2</sup> h °C, wooden formwork: 7 kcal/m<sup>2</sup> h °C. Table V presents the findings of the finite element analysis of the temperature field of the bridge pier structure when various formwork was used.

TABLE V. INFLUENCE OF THE TYPE OF FORMWORK USED ON THE MAXIMUM TEMPERATURE AND MAXIMUM TEMPERATURE DIFFERENCE IN THE BRIDGE PIER STRUCTURE

Type of formwork	Steel formwork	Wooden formwork
$T_{max}$ (°C)	93.45	94.77
$\Delta T$ (°C)	51.74	44.92

The findings of the study indicate that there is no significant or perceptible disparity in the maximum temperature attained at the core of the poured mass when two distinct types of formworks—steel and wooden—are employed. This finding indicates that the selection of formwork material does not exert a substantial influence on the peak temperature attained at the core of the concrete during the curing process. The study suggests that both steel and wooden formwork facilitate a comparable rise in temperature at the core of the concrete mass, irrespective of the material used. However, the study does reveal the occurrence of temperature variations between the surface and the core of the concrete mass, indicating the presence of a temperature gradient within the structure. A comparative analysis of wooden and steel formwork reveals that the temperature differential between the center and the surface of the concrete mass is smaller in the case of wooden formwork. Consequently, the surface temperature of the former is more closely aligned with the central temperature than in the case of the latter. This finding is significant because it suggests that wooden formwork exhibits a distinct thermal behavior compared to steel, which directly influences the temperature distribution within the concrete [19]. The underlying reason for this phenomenon is attributable to the disparity in the thermal properties of the materials. Specifically, wooden formwork exhibits lower thermal conductivity in comparison to steel. Thermal conductivity, defined as a material's capacity to conduct heat, is directly proportional to its efficiency in this regard. In the case of wooden formwork, its reduced thermal conductivity results in less heat transferred away from the concrete mass, enabling a greater proportion of heat to remain within the concrete during the curing process. Consequently, the concrete is exposed to a higher temperature for a longer time, which reduces the temperature difference between the surface and the center. On the other hand, steel formwork, which conducts heat better, helps move heat away from the concrete. This creates a bigger temperature difference between the center and the surface because the heat at the surface can be more easily moved into the air around it. This phenomenon leads to the development of a more pronounced temperature gradient between the inner and outer portions of the concrete

mass. The findings are particularly salient in the context of large-scale concrete constructions, especially during the winter months when temperatures are lower. A notable challenge in such conditions pertains to the potential for the surface of the concrete to cool excessively rapidly when exposed to the cold air. This can cause problems, like thermal cracking, which occurs when the surface gets smaller, while the inside is still warm. It is very important to use materials that can control the temperature of concrete surfaces to prevent these problems. Thus, it is better to use materials that can insulate the concrete surface and stop it from cooling too quickly. In practice, using heat-insulating materials, like polymers, or adding wooden formwork has been identified as a good solution. These materials would create an insulating layer over the surface, helping to keep the concrete warm and prevent it from cooling too fast. These insulation strategies help balance the temperature difference between the core and the surface, which is important for effective curing and preventing surface cracking. The study underscores the significance of selecting the appropriate formwork material when constructing large concrete block structures in cold weather conditions. Ensuring adequate insulation at the surface can markedly enhance the quality and durability of the concrete. This is particularly salient in the context of large block structures, where the volume of concrete leads to a heightened potential for temperature gradients and, consequently, an augmented risk of cracking. Figure 5 provides a detailed graphical representation of the temperature development at both the surface and the center of the concrete pier

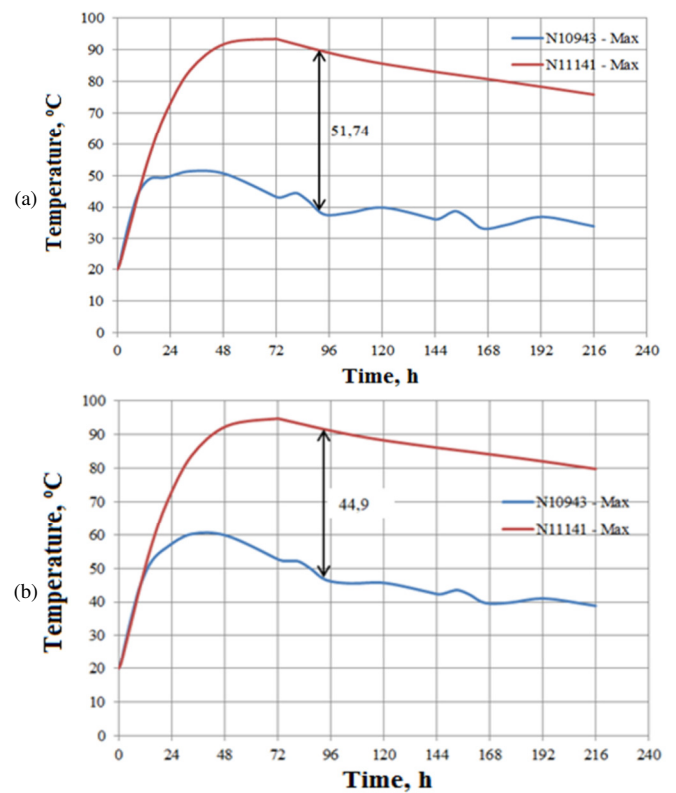


Fig. 5. Temperature evolution at the survey point at the center and surface of the bridge pier in the cases of: (a) steel formwork and (b) wooden

formwork. (N10943: surface of the bridge pier, N11141: center of the bridge pier).

Figure 5 elucidates the temporal evolution of the temperature as the formwork material is transitioned and offers a visual comparison of the temperature gradients for both steel and wooden formwork, highlighting the differences in thermal behavior between the two materials. This analysis underscores the influence that the formwork material can have on the temperature distribution within the concrete, offering valuable insights for improving construction practices and mitigating thermal-related issues during curing.

#### IV. CONCLUSIONS

In consideration of the results obtained, the following observations can be made:

- It is imperative to take into account the factors that influence the temperature and thermal stress fields. In this study, the authors' primary focus was on three factors, namely the cement content, the initial temperature of the concrete mixture, and the type of formwork used. These factors affect both the maximum temperature and the temperature difference between the center and surface of the bridge pier structure during construction.
- The obtained results provide insight into the thermo-mechanical behavior in the context of the bridge pier problem, as well as the heat transfer problem in reinforced concrete structures in general. The survey area, which included 400 kg/m<sup>3</sup>-550 kg/m<sup>3</sup> of cement-containing concrete, was observed, and it was determined that  $T_{max}$  exhibited an increase of 12.46%, equivalent to approximately 12 °C, while the temperature difference  $\Delta T$  value augmented by 17.46%, or 8 °C. Upon examining the initial temperature of the concrete mixture, it was ascertained that the temperature within the concrete block increased by 1 °C for every 1 °C rise in the initial mixture. Consequently, it is rational to reduce the concrete's initial mixture temperature by 15 °C to align with the ambient temperature. This adjustment will result in a 15 °C decrease in the internal structure temperature. The employment of formwork exerts a substantial influence on the maximum temperature  $T_{max}$  and the difference between the temperature minima and maxima ( $\Delta T$ ).
- The usage of wooden formwork is less durable and is not conducive to repeated usage in construction. To mitigate the risk of surface thermal shock and substantial temperature fluctuations, it is imperative to employ wooden and insulated formwork exclusively during winter construction or in conditions where ambient temperatures are low.

#### ACKNOWLEDGEMENT

This research is funded by the University of Transport Technology, Thanh Xuan, Hanoi, Vietnam (UTT), under the grant number DTTD2023-08.

#### REFERENCES

- [1] *ACI 207.1R-96, Mass Concrete*. ACI, 1996.
- [2] *ACI 207.2R-07, Report on Thermal and Volume Change Effects on Cracking of Mass Concrete*. ACI, 2007.
- [3] T.-C. Nguyen, T.-P. Huynh, and V.-L. Tang, "Prevention of crack formation in massive concrete at an early age by cooling pipe system," *Asian Journal of Civil Engineering*, vol. 20, no. 8, pp. 1101–1107, Dec. 2019, <https://doi.org/10.1007/s42107-019-00175-5>.
- [4] D.-P. Pham, T. C. Nguyen, and K.-D. Vu, "The Effect of Thermo-Mechanical Properties of Concrete on the Temperature Field in Mass Concrete," *Engineering, Technology & Applied Science Research*, vol. 14, no. 5, pp. 17209–17213, Oct. 2024, <https://doi.org/10.48084/etasr.8290>.
- [5] *TCVN 9341:2012. Mass concrete - Practice of construction and acceptance*. TCVN, 2012.
- [6] D. Liu, W. Zhang, Y. Tang, and Y. Jian, "Prediction of Hydration Heat of Mass Concrete Based on the SVR Model," *IEEE Access*, vol. 9, pp. 62935–62945, 2021, <https://doi.org/10.1109/ACCESS.2021.3075212>.
- [7] S. Han, Y. Liu, Y. Lyu, J. Liu, and N. Zhang, "Numerical simulation investigation on hydration heat temperature and early cracking risk of concrete box girder in cold regions," *Journal of Traffic and Transportation Engineering (English Edition)*, vol. 10, no. 4, pp. 697–720, Aug. 2023, <https://doi.org/10.1016/j.jtte.2023.05.002>.
- [8] M. Tahersima and P. Tikalsky, "Finite element modeling of hydration heat in a concrete slab-on-grade floor with limestone blended cement," *Construction and Building Materials*, vol. 154, pp. 44–50, Nov. 2017, <https://doi.org/10.1016/j.conbuildmat.2017.07.176>.
- [9] Z. Bofang, *Thermal Stresses and Temperature Control of Mass Concrete*. Oxford, UK: Butterworth-Heinemann, 2014.
- [10] *Guidelines for Control of Cracking of Mass Concrete*. Tokyo, Japan: JCI, 2016.
- [11] T. Kurian and B. Kuriakose, "Numerical analysis of temperature distribution across the cross section of a concrete dam during early ages," *American Journal of Engineering Research (AJER)*, vol. 1, pp. 26–31, 2013.
- [12] M. H. Lee, B. S. Khil, and H. D. Yun, "Thermal Analysis of Hydration Heat in Mass Concrete with Different Cement Binder Proportions," *Applied Mechanics and Materials*, vol. 372, pp. 199–202, 2013, <https://doi.org/10.4028/www.scientific.net/AMM.372.199>.
- [13] Q. Xu, J. M. Ruiz, J. Hu, K. Wang, and R. O. Rasmussen, "Modeling hydration properties and temperature developments of early-age concrete pavement using calorimetry tests," *Thermochimica Acta*, vol. 512, no. 1, pp. 76–85, Jan. 2011, <https://doi.org/10.1016/j.tca.2010.09.003>.
- [14] X. Yu, J. Chen, Q. Xu, and Z. Zhou, "Research on the Influence Factors of Thermal Cracking in Mass Concrete by Model Experiments," *KSCCE Journal of Civil Engineering*, vol. 22, no. 8, pp. 2906–2915, Aug. 2018, <https://doi.org/10.1007/s12205-017-2711-2>.
- [15] Y. Lee and J.-K. Kim, "Numerical analysis of the early age behavior of concrete structures with a hydration based microplane model," *Computers & Structures*, vol. 87, no. 17, pp. 1085–1101, Sep. 2009, <https://doi.org/10.1016/j.compstruc.2009.05.008>.
- [16] L. Yalin, "Finite-Element Modeling of Early-Age Concrete Behavior," Ph.D. dissertation, Auburn University, Auburn, AL, USA, 2018.
- [17] B. E. Byard and A. K. Schindler, "Modeling early-age stress development of restrained concrete," *Materials and Structures*, vol. 48, no. 1, pp. 435–450, Jan. 2015, <https://doi.org/10.1617/s11527-013-0194-2>.
- [18] A. K. Schindler, "Effect of Temperature on Hydration of Cementitious Materials," *ACI Materials Journal*, vol. 101, no. 1, pp. 72–81, 2004.
- [19] N. A. Aniskin, N. T. Chuc, and P. K. Khanh, "The Use of Surface Thermal Insulation to Regulate the Temperature Regime of a Mass Concrete During Construction," *Power Technology and Engineering*, vol. 55, no. 1, pp. 1–7, May 2021, <https://doi.org/10.1007/s10749-021-01310-6>.